JACC: CARDIOVASCULAR IMAGING VOL. 5, NO. 4, 2012

ISSN 1936-878X/$36.00
PUBLISHED BY ELSEVIER INC. DOI:10.1016/j.jcmg.2011.10.008

Molecular Imaging of Human ACE-1 Expression in Transgenic Rats

Vasken Dilsizian, MD,* Todd K. Zynda, DO,† Artiom Petrov, PHD,§
Satoru Ohshima, MD, PHD,† Nobuhiro Tahara, MD, PHD,† Nezam Haider, PHD,§
Amanda Donohue, DO,† Omer Aras, MD,* Frank J. Femia, PHD,‡
Shawn M. Hillier, PHD,‡ John L. Joyal, PHD,‡ Nathan D. Wong, PHD,†
Tomika Coleman, MS,* John W. Babich, PHD,‡ Jagat Narula, MD, PHD§

Baltimore, Maryland; Irvine, California; Cambridge, Massachusetts; and New York, New York

OBJECTIVES The aim of this study was to develop a molecular imaging strategy that can monitor myocardial angiotensin-converting enzyme (ACE)-1 upregulation as a function of progressive heart failure.

BACKGROUND High-affinity technetium-99m–labeled lisinopril (Tc-Lis) has been shown to specifically localize in tissues that express ACE in vivo, such as the lungs. Whether Tc-Lis can also detect upregulation of ACE in the heart, by external in vivo imaging, has not been established.

METHODS Twenty-one ACE-1 over-expressing transgenic (Tg) and 18 wild-type control rats were imaged using in vivo micro single-positron emission computed tomography (SPECT)-computed tomography (CT) at 10, 30, 60, and 120 min after Tc-Lis injection. A subgroup of rats received nonradiolabeled (cold) lisinopril before the Tc-Lis injection to evaluate nonspecific binding. After imaging, the rat myocardium was explanted, ex vivo images were acquired, and percent injected dose per gram gamma-well was counted, followed by an assessment of enzyme-linked immunosorbent assay-verified ACE activity and messenger ribonucleic acid expression.

RESULTS On micro SPECT-CT, myocardial ACE-1 uptake was best visualized in Tg rats at 120 min after Tc-Lis injection. The quantitative uptake of Tc-Lis in the myocardium was 5-fold higher in mutant Tg than in control rats at each time point after tracer injection. The percent injected dose per gram uptake was 0.74 $\pm$ 0.13 in Tg myocardium at 30 min and was reduced substantially to 0.034 $\pm$ 0.003% when pre-treated with cold lisinopril ($p = 0.029$). Enzyme activity assay showed a $>$30-fold higher level of ACE-1 activity in the myocardium of Tg rats than in controls. The ACE-1 messenger ribonucleic acid was quantified, and lisinopril was found to have no effect on ACE-1 gene expression.

CONCLUSIONS The Tc-Lis binds specifically to ACE, and the activity can be localized in Tg rat hearts that over-express human ACE-1 with a signal intensity that is sufficiently high to allow external imaging. Such a molecular imaging strategy may help identify susceptibility to heart failure and may allow optimization of pharmacologic intervention. (J Am Coll Cardiol Img 2012;5:409–18) © 2012 by the American College of Cardiology Foundation

From the *Department of Diagnostic Radiology and Nuclear Medicine, University of Maryland School of Medicine, Baltimore, Maryland; †Division of Cardiology, University of California, Irvine, Irvine, California; ‡Molecular Insight Pharmaceuticals,

JACC: CARDIOVASCULAR IMAGING, VOL. 5, NO. 4, 2012
APRIL 2012:409–18

The renin-angiotensin system is activated early in the failing heart with angiotensin-converting enzyme (ACE)-1 activity upregulated within the cardiomyocytes (1,2). Left ventricular ACE expression has been found to be significantly enhanced in the failing human myocardium in proportion to the increasing disease severity, regardless of the underlying etiology of heart failure (3). Although serum renin-angiotensin activity often returns to relatively normal levels in well-compensated heart failure, tissue renin-angiotensin activity may remain elevated in the myocardium and may contribute significantly to the progression of myocardial remodeling (4–6).

See page 419

ABBREVIATIONS AND ACRONYMS

ACE = angiotensin-converting enzyme

cDNA = cardiac deoxyribonucleic acid

CT = computed tomography

mRNA = messenger ribonucleic acid

%ID/g = percent injected dose per gram

PET = positron emission tomography

SPECT = single-positron emission computed tomography

Tc-Lis = technitium-99m–labeled lisinopril

Tg = transgenic

The cardiac renin-angiotensin system has also been shown to correlate with the extent of cardiac hypertrophy (7), cardiac fibrosis (8), and myocyte apoptosis (9). This implies a role of local tissue effects of renin-angiotensin activity on left ventricular remodeling and, importantly, provides an opportunity for imaging local ACE activity in the myocardium using external molecular imaging probes with positron emission tomography (PET) or single-positron emission computed tomography (SPECT).

Large clinical trials using ACE inhibitors have shown to improve patient mortality, reduce hospitalizations for heart failure, attenuate left ventricular remodeling, and improve quality of life (6,10,11). Consequently, ACE inhibition has become central to the treatment of patients with heart failure, left ventricular dilation and remodeling after myocardial infarction, endothelial dysfunction, and diabetic nephropathy. However, there is significant interindividual variability in response to ACE therapy, and at present, there is no reliable method that predicts the response of an individual patient to ACE inhibition. Factors such as genetic differences, sex, race, comorbid conditions, age, concomitant medications, renal and liver functions are all important determinants of individual response to ACE inhibitors. It is conceivable, therefore, that the knowledge of imaged-guided myocellular ACE-1 expression would allow tailoring medical therapy to individual needs (12,13).

The myocellular ACE upregulation has been successfully targeted with F-18 labeled fluorobenzoyl-lisinopril in ex vivo myocardial samples obtained from explanted cardiomyopathic hearts in cardiac allograft recipients (14–16). In the present study, we used technetium-99m–labeled lisinopril (Tc-Lis), as a molecular probe, to determine the feasibility for external in vivo imaging of ACE-1 expression in human ACE-1 over-expressing transgenic (Tg) rats by hybrid micro SPECT-CT. The clinical implications of this project will be to better define the complex biochemical phenomena underlying cardiac remodeling and heart failure. If the intensity of the Tc-Lis binding signal is sufficiently high in the heart of Tg rats, it will support subsequent noninvasive imaging studies in human subjects with heart failure using external SPECT imaging to assess remodeling myocardium. Our hypothesis is that the intensity of the Tc-Lis signal as measured by percent injected dose per gram (%ID/g) uptake would be increased in the heart of Tg rats after Tc-Lis administration, but decreased if pre-treated with nonradiolabeled (cold) lisinopril.

METHODS

Study protocol. Twenty-one ACE-1 over-expressing Tg rats and 18 wild-type Sprague-Dawley control rats were studied. The Tg rats were obtained from Charité University (Campus Benjamin Franklin, Berlin, Germany); this Tg rat model has been described previously (2). A 2.1 kb rat myosin light chain (rMLC-2) promoter has been used to direct cardiac-specific expression of human ACE-1 cardiac deoxyribonucleic acid (cDNA) (18). The Tg rats (L1173 strain) maintain up to 50-fold selective over-expression of human ACE-1 in ventricles. All Tg and control rats were males and similarly aged. The ACE-1 targeting imaging agent was developed by Molecular Insight Pharmaceuticals, Inc. (Cambridge, Massachusetts), which is a high-affinity analog of lisinopril containing a tridentate chelate and radiolabeled with ^{99m}Technetium (^{99m}Tc). This compound localizes in the tissues that express ACE abundantly, and the technique has been reported previously (19). The experimental protocol was

Cambridge, Massachusetts; and the §Zena and Michael A. Weiner Cardiovascular Institute, Mount Sinai School of Medicine, New York, New York. Dr. Dilsizian is a consultant to and has received research funding from Molecular Insight Pharmaceuticals. Dr. Babich is an employee of Molecular Insight Pharmaceuticals. All other authors have reported they have no relationships relevant to the contents of this paper to disclose. H. William Strauss, MD, served as Guest Editor for this paper.

Manuscript received September 23, 2011; accepted October 3, 2011.

approved by the Animal Care and Use Committee of the University of California, Irvine, School of Medicine. Noninvasive images were obtained using a dual-head micro-SPECT gamma camera combined with micro-CT (X-SPECT, Gamma Medica, Inc., Northridge, California). The SPECT images of the heart were acquired in a 64 × 64 matrix, 32 stops at 15 s per stop at 140 keV photopeak of ^{99m}Tc with 15% windows using a low-energy, high-resolution, parallel-hold collimator. Immediately after SPECT imaging, a micro-CT scan was acquired using an X-ray tube operating at 50 kVp and 0.8 mA. Images were captured for 2.5 s per view for 256 views in 360-degree rotation. After transferring to a 256 × 256 matrix, the micro-SPECT images and micro-CT studies were fused, allowing scintigraphic and anatomic in vivo images in all tomographic scans in the 3 different spatial axes.

Radionuclide imaging with Tc-Lis. Micro SPECT-CT images were obtained at 10, 30, 60, and 120 min after Tc-Lis administration. Each rat was injected with approximately 3 mCi Tc-Lis. Nine of 21 Tg rats and 8 of 18 control rats received 0.6 mg/kg cold lisinopril 5 min before radiotracer administration. After in vivo imaging, the rat myocardium was explanted, and static ex vivo images were acquired for 15 min using a low- energy, high-resolution, parallel-hole collimator. Subsequently, anesthetized animals were euthanized by carbon dioxide asphyxiation at 10, 30, 60 and 120 min to evaluate tissue tracer biodistribution. The %ID/g was gamma-well counted. Biodistribution of Tc-Lis in heart, lung, liver, spleen, kidney, and blood was determined.

Biochemical evaluation of myocardial specimens. The ACE-1 gene expression and enzyme activity were quantified in the myocardium of control rats and ACE-1 over-expressing Tg rats. Myocardial samples were collected from untreated and lisinopril pre-treated control and Tg rats after in vivo and ex vivo imaging. Samples were frozen in liquid nitrogen and stored at −70° C until used. Protein isolation was performed, and ACE-1 enzyme activity was quantified. Myocardial tissues were homogenized in lysis buffer (50 mM Tris-HCI pH 7.6, 150 mM NaCl, 1 mM sodium vandate, 0.1 mM Phenylmethylsulfonyl fluoride, 10 μg/ml aprotinin/leupeptin/pepstatin A, 1% NP-40, 1 mM DL-Dithiothreitol) and kept in ice for 30 min. Homogenate was centrifuged at 10,000 *g* for 15 min at 4° C, and supernatant cytosolic fraction was collected for ACE-1 assay. Protein concentrations of all the samples were determined using Bio-Rad protein assay reagent (Bio-Rad Laboratories, Hercules, California) and equalized. The ACE activity was determined by ACE colorimetric enzymatic assay (ALPCO Diagnostics, Schonenbuch, Switzerland). This procedure utilizes the cleavage of a synthetic substrate, N-hippuryl-histidyl-l-leucine, into hippuric acid and the dipeptide histidyl-leucine (18,20) by ACE. Released hippuric acid was complexed with cyanuric chloride, and the absorbance was measured at 382 nm. One unit of ACE activity is defined as the amount of enzyme required to release hippuric acid, 1 $\mu mol \cdot min^{-1} \cdot l^{-1}$ serum, at 37° C. The standard curve was obtained from the absorbance of each standard (serial dilutions of the hippuric acid from 2,500 to 250 μmol/l) at 382 nm. Cardiac tissue samples from Sprague-Dawley control rats and Tg rats were assayed in duplicate for ACE levels. Positive control serum with a known ACE level was included for quality assurance. Quantification of ACE-1 gene expression was performed by performing RNA isolation, cDNA synthesis, and a gene expression assay. Total RNA was extracted from myocardial tissues using the RNeasy Midi Kit (Qiagen, Valencia, California) according to the manufacturer's protocol. The amount of RNA was measured by absorbance at 260 nm. Integrity of RNA was verified by electrophoresis and by a 260/280 nm absorption ratio. Total RNA was reverse transcribed into first-strand cDNA using the SuperScript III RT kit (Invitrogen Inc., Carlsbad, California) according to the manufacturer's instructions. Briefly, 5 μg total RNA was added to 1 μl oligo (dT), 1 μl 10 mM Deoxynucleotide set [2′-Deoxyadenosine 5′-triphosphate; 2′-Deoxycytidine 5′-triphosphate; 2′-Deoxyguanosine 5′-triphosphate; Thymidine 5′-triphosphate] (dNTPs), 2 μl 10 × first strand buffer, 4 μl 25 mM $MgCl_2$, 2 μl 0.1 M DL-Dithiothreitol, and 1 μl RNAase out. First, RNA, oligo (dT), and dNTPs were mixed and incubated at 65° C for 5 min for annealing and then chilled on ice until the other components were added. The samples were incubated at 42° C for 2 min. Then 1 μl SuperScript III (40 U/μl) was added, and the samples were incubated at 42° C for 50 min. The reaction was inactivated at 70° C for 15 min. The samples were kept on ice, centrifuged briefly, added to 1 μl of RNAse H, and incubated at 37° C for 20 min. Quantification of gene expression was carried out using cDNA samples. Pre-designed and validated, using ACE-1 gene-specific TaqMan gene expression assay (ID: Rn00561094_m1 from Applied Biosystems, Foster City, California) was used in duplicate, according to the manufacturer's protocol.

The level of glyceraldehyde 3-phosphate dehydrogenase (TaqMan gene expression assay ID: Rn99999916_s1) was used as endogenous control for data normalization. Real-time quantitative polymerase chain reaction was performed on an ABI PRISM 7000 SDS (Applied Biosystems) using 2.5 μl (20× concentration) TaqMan gene expression assay (Applied Biosystems) in a total volume of 50 μl, using 25 μl 2XTaqMan gene expression polymerase chain reaction master mix, 1 μl cDNA. Cycle conditions were 50° C for 2 min, 95° C for 10 min, followed by 40 cycles at 95° C for 15 s and 60° C for 1 min. Each sample was tested in duplicate, and a sample without template was included as a negative control. Relative quantification was made from collected threshold cycle numbers data. Relative expression levels of ACE-1 mRNA were normalized according to GAPDH expression using the 2-ΔΔCT method (21).

Statistical analyses. Quantitative radiotracer uptake was calculated as %ID/g of the tissue. Radiotracer uptake measurements were expressed as mean ± SD. The exact Mann-Whitney *U* test was used for pairwise comparison of %ID/g in groups. One-sided p values (based on our hypothesis of expected increases in uptake from Tc-Lis administration and decreases from cold lisinopril pre-treatment) were calculated, and p values <0.05 were considered statistically significant. The SAS statistical software, version 9.1.3 (SAS Institute, Cary, North Carolina), was used to conduct all analyses and computation of the comparisons of radiotracer uptake measurements in groups.

RESULTS

In vivo imaging of cardiac ACE over-expression. Simultaneous micro SPECT-micro-CT acquisition provided scintigraphic and anatomic images, and allowed comparison of myocardial uptake of Tc-Lis within Tg rats and control rats in vivo. Examples of in vivo images are shown in Figure 1. In a control rat, micro SPECT-CT images acquired 60 min after Tc-Lis administration displays tracer uptake in the lungs (Fig. 1, white arrowhead) but not in the myocardium (Fig. 1, left panel, yellow arrow), suggesting normal ACE activity in the lungs and a lack of appreciable ACE activity in normal myocardium. Conversely, the ACE-1 over-expressing Tg rats demonstrated substantial tracer uptake within

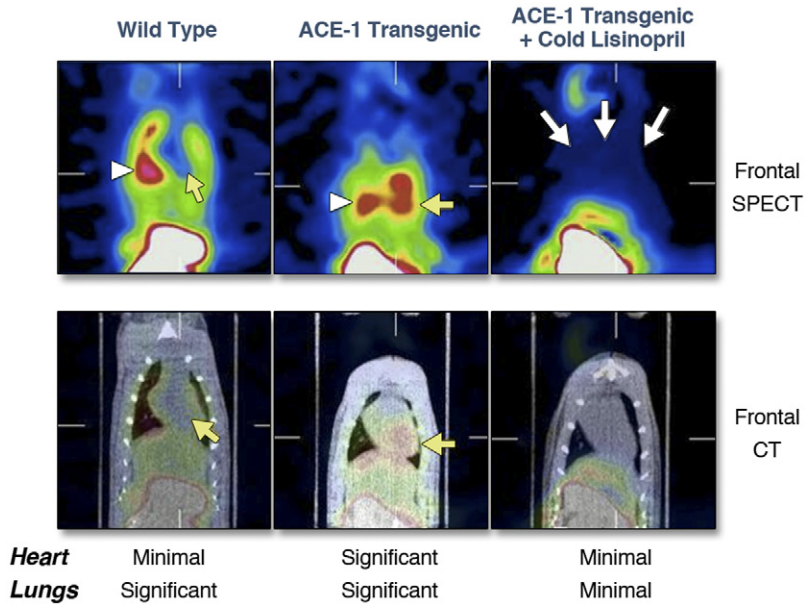

Figure 1. Noninvasive Micro SPECT-CT Imaging of ACE-1 Activity

Micro single-positron emission computed tomography (SPECT)-computed tomography (CT) imaging provides simultaneous scintigraphic and morphologic localization of technitium-99m–labeled lisinopril uptake, 60 min after tracer administration, in a control animal **(left)**, angiotensin-converting enzyme (ACE)-1 over-expressing transgenic animal **(middle)**, and a transgenic animal after cold lisinopril administration **(right)**. **White arrowhead** demonstrates intense lung uptake, and **yellow arrows** point to myocardial ACE-1 activity. **White arrows** suggest a substantial reduction in tracer uptake after pre-treatment with nonradiolabeled lisinopril administration. Despite the several-fold lower lung-to-heart ratio in the transgenic animals when compared to the control animals, the lung uptake may still be visualized and, may contribute spillover counts to the myocardium, which can be corrected for.

the myocardium (Fig. 1, middle panel, yellow arrow) and lungs (white arrowhead) after Tc-Lis administration. Pre-treatment of the ACE-1 over-expressing Tg rats with nonlabeled cold lisinopril almost completely abolished the radiotracer uptake within the myocardium and lungs (Fig. 1, right panel, white arrows), demonstrating targeting specificity of the radiotracer. Noninvasive micro SPECT-CT imaging studies, therefore, demonstrated the feasibility of Tc-Lis based targeting of the ACE-1 expression within the myocardium.

Ex vivo imaging of cardiac ACE over-expression and quantitative %ID/g uptake of Tc-Lis in myocardium. Ex vivo imaging of cardiac ACE at different time points within the individual rats in different groups is demonstrated in Figure 2. It is important to note that the quantitative uptake of Tc-Lis in the myocardium was 5-fold higher in mutant Tg rats than in control rats at each time point after tracer injection.

Quantitative myocardial uptake of Tc-Lis at various time points is shown in the bar graph in Figure 2 (right). Although maximum myocardial uptake was seen at 30 min, best target-to-background ratio was observed at 120 min because of significant Tc-Lis clearance of ACE from the circulation and the pulmonary region. Administration of nonradiolabeled lisinopril 5 min before Tc-Lis administration significantly reduced the myocardial Tc-Lis uptake. The %ID/g uptake in Tg and control rats at 10 min was 0.48 ± 0.29% and 0.19 ± 0.10% ($p = 0.171$), respectively; and at 30 min, it was 0.74 ± 0.13% and 0.17 ± 0.03% ($p = 0.028$). The uptake reduced substantially in Tg rats pre-treated with cold lisinopril; %ID/g at 10 min was reduced to 0.037 ± 0.015% ($p = 0.014$), and at 30 min, it was reduced to 0.034 ± 0.003% ($p = 0.028$). Uptake values in control rats were quite low to begin with and remained low with cold lisinopril pre-treatment (0.05 ± 0.01% at 10 min and 0.049 ± 0.008% at 30 min, $p = 0.014$ for both time points). Moreover, the uptake of Tc-Lis at 10 min or 30 min after cold lisinopril pre-treatment was comparable for Tg rats and control rats.

Biodistribution of Tc-Lis in organs. Biodistribution of Tc-Lis in all visceral organs and blood was calculated (Table 1). The Tc-Lis uptake did not significantly differ between any groups in blood or various organs. The maximum radiation burden was observed for lungs at all time points; for instance, %ID/g uptake of 8.6 ± 1.6% and 9.5 ± 2.6% ($p = 0.243$) was seen in Tg rats and control rats, respectively, at 30 min. Administration of cold lisinopril substantially reduced lung uptake to 0.04 ± 0.02 ($p = 0.014$) in Tg rats and 0.07 ± 0.02 ($p = 0.014$) in control animals, at 30 min. Kidney, spleen, and liver were the other organs with high tracer uptake (Table 1).

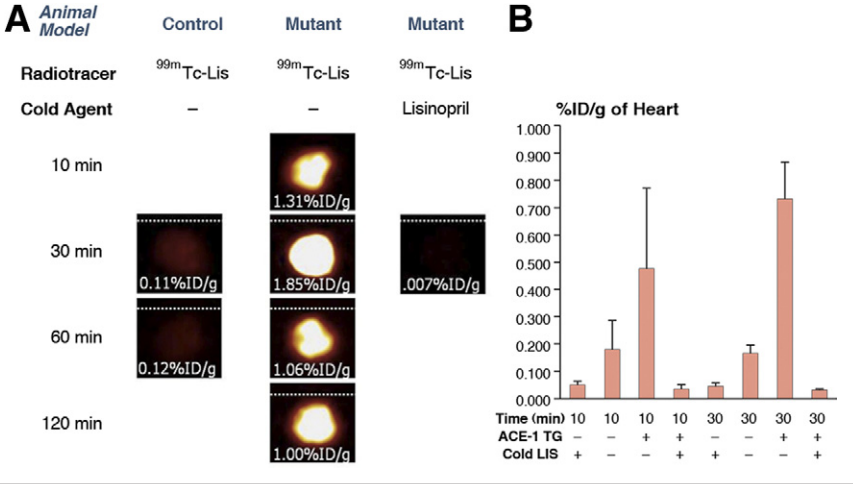

Figure 2. Ex Vivo Imaging of Explanted Hearts at Various Time Points in Representative Animals and Quantitative Tracer Uptake in Myocardium

(A) Radiotracer uptake is demonstrated in a control rat **(left)**, transgenic rats **(middle)**, and a transgenic rat after unlabeled lisinopril **(right)** at different time points. Uptake is significantly higher at each time point in transgenic rats. The radiotracer uptake is substantially decreased after simultaneous administration of cold tracer for competitive uptake inhibition of the radiotracer. **(B)** Quantitative ^{99m}Tc-labeled lisinopril uptake in larger number of animals demonstrates the same observation. ACE = angiotensin-converting enzyme; LIS = lisinopril; %ID/g = percent injected dose per gram; ^{99m}Tc-Lis = technitium-99m–labeled lisinopril; TG = transgenic.

JACC: CARDIOVASCULAR IMAGING, VOL. 5, NO. 4, 2012
APRIL 2012:409–18

Table 1. Radiotracer Biodistribution in Target and Non-Target Organs at Various Time Points and With or Without Competitive Inhibition

Organ	15 Min	30 Min	60 Min	120 Min
Heart				
Control		0.110	0.120	
RL-LSP	1.308	1.849	1.060	1.003
Cold LSP		0.007		
Lung				
Control		7.925	8.535	
RL-LSP	8.844	10.757	9.754	4.581
Cold LSP		0.014		
Liver				
Control		0.331	0.369	
RL-LSP	0.622	0.483	0.565	0.159
Cold LSP		0.102		
Spleen				
Control		0.449	0.777	
RL-LSP	0.529	0.550	0.535	0.118
Cold LSP		0.011		
Kidney				
Control		0.217	0.314	
RL-LSP	1.700	1.627	1.402	1.586
Cold LSP		0.105		
Blood				
Control		0.032	0.028	
RL-LSP	0.063	0.058	0.062	0.045
Cold LSP		0.016		

LSP = lisinopril; RL = radiolabeled.

Biochemical and molecular characterization of ACE-1 expression and activity. Enzyme activity assays indicated a >30-fold higher level of ACE-1 in the myocardium of ACE-1 over-expressing Tg rats as compared to control animals. Nonradiolabeled lisinopril (0.6 mg/kg) pre-treatment for 30 min decreased the ACE-1 activity in these hearts to a level similar to that of controls (Fig. 3, left). The quantitative uptake of Tc-Lis in the myocardium, which was higher in Tg rats than in control rats at each time point between 10 min and 120 min after tracer injection, paralleled the measured ACE-1 activity. These findings demonstrate that the imaging data are truly representative of the myocardial biochemistry, and the response to the cold-lisinopril demonstrates the specificity of the targeting radiotracer.

Conversely, expression of ACE-1 mRNA by relative quantification TaqMan assay shows a 2-fold increase in over-expressing Tg rat heart compared to control rats (Fig. 3, right). Unlike ACE-1 enzymatic activity, mRNA level showed no decrease in response to cold lisinopril pre-treatment in either Tg hearts or control hearts. These results indicated that lisinopril, as expected, would not influence the overall mRNA expression, but will elicit a profound effect on enzyme activity.

DISCUSSION

Left ventricular remodeling, characterized by changes in chamber size, shape, and function, contributes to heart failure. Systemic and local neurohumoral factors are known to play major roles in the process of left ventricular remodeling, and among them the renin-angiotensin system occupies a central place. Blockade of the renin-angiotensin system, by ACE inhibitors, angiotensin II type 1

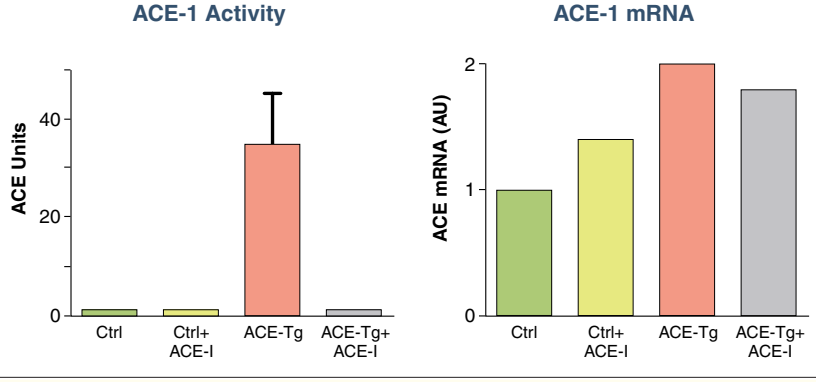

Figure 3. Tracer Uptake, ACE-1 Message Expression and Enzyme Activity

Enzyme activity assays **(left)** indicates a >30-fold higher level of angiotensin-converting enzyme (ACE)-1 activity in the myocardium of ACE-1 over-expressing transgenic (Tg) rats as compared to control (Ctrl) animals. The activity is markedly reduced after nonradiolabeled lisinopril (0.6 mg/kg) pre-treatment and confirms the imaging data. Conversely, expression of ACE-1 messenger ribonucleic acid (mRNA) by relative quantification TaqMan assay shows a 2-fold increase in over-expressing Tg rat heart compared to controls **(right)**. Unlike ACE-1 enzymatic activity, mRNA level showed no decrease in response to cold lisinopril pre-treatment.

receptor blockers, or aldosterone antagonists has been shown to be effective in preventing or reversing left ventricular remodeling. Although numerous clinical trials have demonstrated a direct beneficial effect of renin-angiotensin blockade on patient outcome in heart failure, in many of these trials, significant differences have been observed in clinical responses of various subpopulations to ACE inhibitors. Although some clinical and laboratory parameters may help predict the response of patients to renin-angiotensin blockade, since the tissue component of the renin-angiotensin system is not directly accessible, they lack accuracy. Conversely, external cardiac imaging using radiolabeled probes of the renin-angiotensin system may give a direct measure of tissue ACE expression in the myocardium. Hence, targeted molecular imaging of cardiac ACE-1 and the remodeling process may provide valuable insight into the natural progression of heart failure, which could allow earlier and more effective intervention. Although pharmacologic ACE inhibition is a common therapy for heart failure, the cellular response with such therapy on an individual basis may be variable, and assessment of tissue ACE activity may allow optimization of therapeutic intervention.

ACE-1 is a large type I anchored glycoprotein that spans the cell membrane (22,23). It contains 2 distinct extracellular catalytic binding sites (24), and a number of auxiliary binding subsites (25). It acts as a zinc metalloproteinase that transforms the short peptide substrate angiotensin I to the more physiologically active angiotensin II peptide (22) and degrades bradykinin (23). ACE inhibitors bind to these extracellular enzyme binding sites specifically with varying affinity (25,26). Radiolabeled Tc-Lis likely binds to extracellular binding sites located along the myocardial cell membrane (Fig. 4).

Molecular imaging of myocardial ACE-1. The present study demonstrates the feasibility of external noninvasive in vivo imaging of cardiac tissue ACE-1 by hybrid micro SPECT-CT. Enzyme activity assay indicated a >30-fold higher level of ACE-1 in the myocardium of Tg rats as compared to control rats. The quantitative uptake of Tc-Lis closely correlated the enzyme activity demonstrating the accuracy of the molecular imaging strategy. Cold lisinopril (0.6 mg/kg) treatment before radiolabeled lisinopril administration decreased the ACE-1 activity and the tracer uptake, establishing the specificity of the radioisotope probe to myocardial ACE-1. The development of such molecular imaging strategy for assessing ACE-1 upregulation in the heart that can monitor ACE as a function of progressive heart failure by external imaging may lead to a new generation of molecular imaging probes for monitoring disease progression and the effectiveness of treatments for heart failure. Data correlating cardiac ACE-1 imaging to clinical outcomes will ultimately be necessary.

Previous reports of molecular imaging in remodeling process. In vivo noninvasive imaging of angiotensin II receptors has been successfully demonstrated in the remodeling post-infarction myocardium, with uptake occurring almost exclusively in the myofibroblasts (27–30). Radiolabeled ^{99m}Tc–labeled Cy5.5 arginine-glycine-aspartic acid (RGD) imaging peptide (CRIP) evaluated the extent of myofibroblast prevalence within post-myocardial infarction mice, and demonstrated an ability to evaluate

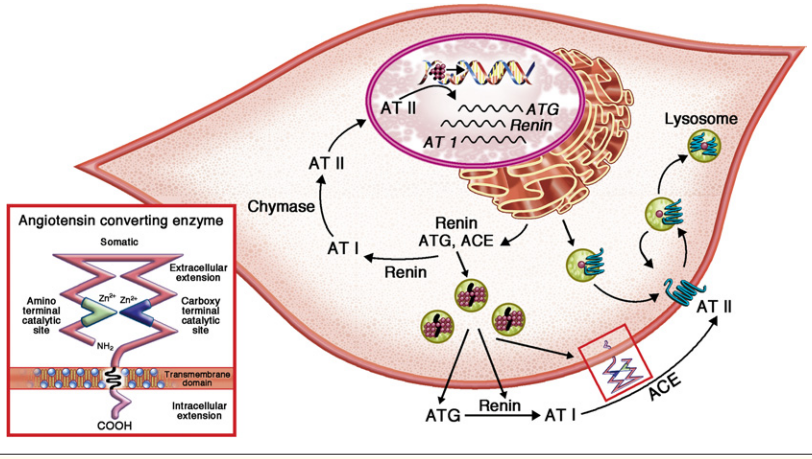

Figure 4. Diagrammatic Representation of Cell Surface ACE-1 and Potential Targeting by Radiolabeled Lisinopril

Modified from Kumar et al. (4) and Dzau et al. (24). ACE = angiotensin-converting enzyme; ATG = angiotensin; AT I = angiotensin I; AT II = angiotensin II.

JACC: CARDIOVASCULAR IMAGING, VOL. 5, NO. 4, 2012
APRIL 2012:409–18

the efficacy of therapy with angiotensin-aldosterone axis suppression using molecular noninvasive imaging (28,29). The CRIP uptake was attenuated by therapy with captopril alone or in combination with losartan [28], and diminished radiotracer uptake was associated with systolic function preservation (29). In another study, in vivo noninvasive imaging of angiotensin II type 1 receptors utilizing ^{99m}Tc-losartan successfully demonstrated remodeling myocardium of post-infarction mice, with uptake occurring again almost exclusively in the myofibroblast (27). Although the extent of angiotensin II uptake, and hence the magnitude of fibroblastic proliferation, should predict ultimate interstitial fibrosis and remodeling, it may be advisable to evaluate the neurohumoral perturbations at the myocyte level that precedes proliferation of myofibroblasts.

Transglutaminase factor XIII is a key enzyme in myocardial remodeling post-infarction, and is involved in extracellular matrix turnover and regulation of inflammation after ischemic injury (31). In another molecular imaging study, factor XIII was assessed in healing myocardium using a post-myocardial infarction murine model utilizing ^{111}Indium-labeled affinity peptide and micro SPECT-CT (32). The radioisotope cross-links to extracellular matrix proteins, allows direct assessment of wound healing in vivo and predicts prognosis post-myocardial infarction (32). Increased cardiac ACE-1 activity likely has significant influence on cardiac hypertrophy augmentation, and potentially represents a risk factor in persons with heart failure or in persons predisposed to develop heart failure. The ability to visualize alterations in the expression of angiotensin I and ACE-1, and myocardial factor XIII levels in the failing heart in vivo may facilitate pharmacologic-induced cessation of adverse cardiac remodeling.

ACE inhibitors with high versus low degrees of tissue penetration. A trial specifically designed to compare outcomes among cardiac patients prescribed ACE inhibitors with high versus low degrees of tissue penetration has not been conducted. Most studies have focused on comparisons of particular ACE inhibitor with placebo. Although results from a few head-to-head trials suggest that various ACE inhibitors are associated with similar reductions in mortality (33), there are, however, other head-to-head trials and observational studies that provide evidence to the contrary (34–37). In a recent publication, using linked hospital discharge and prescription claims databases in 3 provinces of Canada, the investigators identified 43,316 patients with heart failure who were 65 years of age or older and filled prescriptions for ACE inhibitors within 30 days after discharge from hospital (38). The mean follow-up period was 2.1 years, and none of the patients was admitted for heart failure in the 3 years before the study period. Such "real-world" analysis, albeit retrospective and observational, provided important comparative information for 8 different ACE inhibitors with variable high and low degrees of tissue penetration that would not be readily available in a clinical trial. The results showed that captopril and enalapril (low tissue penetration ACE inhibitors) were associated with about 10% to 15% higher mortality than ramipril (high tissue penetration ACE inhibitor). Lisinopril patients did not have a significantly different mortality from that of patients who were receiving ramipril. Moreover, in a prior randomized trial comparing lisinopril and captopril in heart failure patients, lisinopril improved nonfatal outcomes such as exercise duration in subgroups of patients when compared to captopril (34).

The potential impact of other ACE inhibitors with different affinities on lisinopril binding. Although ACE inhibitors share the same basic structure, there are important structural and pharmacologic differences within the class that influence the potency and bioavailability of the drug and may explain some of the variation in their effectiveness in the literature. Conversely, whereas affinities of ACE inhibitors vary, they are relatively close to each other, within a factor of 10-fold. It is important to point out, however, that it is the mass amount of the compound, not just the affinity, that impacts ACE saturation. Given the large disparity between the mass of the compound administered relative to the differences in the individual affinities of various ACE inhibitors, the affinity is not likely to significantly influence the ultimate image interpretation. As a result, we expect that the lisinopril radioligand will be measuring unoccupied enzymes.

For new-onset heart failure patients, the goal would be to acquire pre-ACE therapy lisinopril SPECT and repeat the imaging study after ACE inhibitor therapy. That would be consistent with occupancy studies that were first carried out in humans with drugs for neurologic diseases, given that plasma levels are not indicative of occupancy. If the lisinopril signal is blocked on post-ACE scan or there is very little uptake when compared to the pre-ACE scan, then the therapeutic dose of ACE is appropriate. That would represent paired studies and be consistent with the concept of individualized

medicine. However, if a heart failure patient is already receiving an ACE inhibitor, and a pre-ACE scan cannot be obtained, then the lisinopril signal could be compared to a group database. That is, in subsequent early clinical phase studies, healthy subjects can be studied to set a parameter of normal criteria for ACE availability, such as standardized uptake value or change in % ID/g. Such a parameter would then be utilized to assess ACE occupancy on a group basis and compare the post-ACE scan of the heart failure patient to the group base derived parameter (e.g., standardized uptake value threshold). This approach has been used routinely in measurement of glucose metabolism in cancer patients.

Spillover of counts from ACE activity in the lungs into the myocardium. The circulating renin-angiotensin system is initiated by the release of renin from the kidney, which acts in circulating blood on angiotensinogen of hepatic origin to produce angiotensin I, which, in turn, is modified to angiotensin II through enzymatic action of the ACE predominantly in the pulmonary circulation. As such, constitutive lung ACE activity may spill over into the myocardium during image acquisition. However, spillover is a problem that can be overcome (39–41). Many techniques have been developed and published over the years to correct the equally severe problem of spillover of counts from the left ventricular cavity into the myocardium, during kinetic modeling of the heart (e.g., ammonia, rubidium, water PET imaging). Accordingly, there are several possible corrections that could be performed. For example, in the era of hybrid PET-CT and SPECT-CT, the lung/myocardial borders could first be drawn on the CT, and then the lung region can be set to a constant value equal to whatever the average counts were in the SPECT or PET lungs, leaving the myocardium zero. Then the image can be blurred with the known resolution of the imaging device, PET or SPECT. The myocardial region can then be placed on this artificial, CT-based image, and determine how many counts are in the myocardial region. This value is the value that needs to be subtracted from the actual measured PET or SPECT myocardial region. Alternatively, very small amount of macro-aggregated albumin could be injected, which is clinically used for lung perfusion studies, to find out how many counts spilled into the myocardium. Very low doses are needed, because we are not interested in a good lung image, only in finding out how many counts spilled into the myocardium.

CONCLUSIONS

Tc-Lis binds specifically to ACE, and the activity can be localized in Tg rat hearts that over-express human ACE-1. Moreover, the intensity of the Tc-Lis binding signal is sufficiently high to allow external in vivo imaging by hybrid micro SPECT-CT. Because ACE is upregulated in remodeling human myocardium, it is expected that such a molecular imaging strategy will help identify patients susceptible to heart failure development and may allow optimization of pharmacologic intervention.

Acknowledgments

The imaging agent (Tc-Lis) was kindly provided by Molecular Insight Pharmaceuticals, Cambridge, Massachusetts.

Reprint requests and correspondence: Dr. Vasken Dilsizian, University of Maryland Medical Center, Department of Diagnostic Radiology and Nuclear Medicine, 22 South Greene Street, Room N2W78, Baltimore, Maryland 21201-1595. *E-mail: vdilsizian@umm.edu.*

REFERENCES

1. Paul M, Pinto YM, Schunkert H, Ganten D, Böhm M. Activation of the renin-angiotensin system in heart failure and hypertrophy—studies in human hearts and transgenic rats. Eur Heart J 1994;15:63–7.
2. Tian XL, Pinto YM, Costerousse O, Franz WM, et al. Over-expression of angiotensin converting enzyme-1 augments cardiac hypertrophy in transgenic rats. Hum Molec Genetics 2004;13:1441–50.
3. Studer R, Reinecke H, Müller B, Holtz J, Just H, Drexler H. Increased angiotensin-I converting enzyme gene expression in the failing human heart. Quantification by competitive RNA polymerase chain reaction. J Clin Invest 1994;94:301–10.
4. Kumar R, Singh V, Baker KM. The intracellular renin-angiotensin system: implications in cardiovascular remodeling. Curr Opin Nephrol Hypertens 2008;17:168–73.
5. Yamagishi H, Kim S, Nishikimi T, Takeuchi K, Takeda T. Contribution of cardiac renin-angiotensin system to ventricular remodeling in myocardial-infarcted rats. J Mol Cell Cardiol 1993;25:1369–80.
6. Pfeffer MA, Braunwald E, Moyé LA, et al. Effect of captopril on mortality and morbidity in patients with left ventricular dysfunction after myocardial infarction. Results of the survival and ventricular enlargement trial. The SAVE Investigators. N Engl J Med 1992;327:669–77.
7. Schunkert H, Dzau V, Tang SS, Hirsch AT, Apstein CS, Lorell BH. Increased rat cardiac angiotensin converting enzyme activity and mRNA expression in pressure overload left ventricular hypertrophy. Effects on coronary resistance, contractility, and relaxation. J Clin Invest 1990;86:1913–20.

8. Weber KT, Brilla C. Pathological hypertrophy and cardiac interstitium. Fibrosis and renin-angiotensin-aldosterone system. Circulation 1991;83:1849–65.
9. Anversa P, Cheng W, Liu Y, Leri A, Redaelli G, Kajstura J. Apoptosis and myocardial infarction. Basic Res Cardiol 1998;98:8–12.
10. The SOLVD Investigators. Effect of enalapril on survival in patients with reduced left ventricular ejection fractions and congestive heart failure. N Engl J Med 1991;325:293–302.
11. The CONSENSUS Trial Study Group. Effects of enalapril on mortality in severe congestive heart failure. Results of the Cooperative North Scandinavian Enalapril Survival Study (CONSENSUS). N Engl J Med 1987;316:1429–35.
12. Baliga R, Narula J. Pharmacogenomics of congestive heart failure. Med Clin North Am 2003;87:569–78.
13. Taylor AL, Ziesche S, Yancy CW, et al. Combination of isosorbide dinitrate and hydralazine in blacks with heart failure. N Engl J Med 2004;351:2049–57.
14. Dilsizian V, Eckelman WC, Loredo ML, Jagoda EM, Shirani J. Evidence for tissue angiotensin-converting-enzyme in explanted hearts of ischemic cardiomyopathy using targeted radiotracer technique. J Nucl Med 2007;48:182–7.
15. Chandrashekhar Y, Narula J. Exposing ACE up the sleeve. J Nucl Med 2007;48:173–4.
16. Lee YHC, Kiesewetter DO, Lang L, et al. Synthesis of 4-[18F]fluorobenzoyllisinopril: a radioligand for angiotensin-converting enzyme (ACE) imaging with positron emission tomography. J Label Cpd Radiopharm 2001;44 Suppl:268–70.
17. Hwang DR, Eckelman WC, Mathias CJ, Petrillo EW Jr., Lloyd J, Welch MJ. Positron-labeled angiotensin-converting enzyme (ACE) inhibitor: fluorine-18- fluorocaptopril—probing the ACE activity in vivo by positron emission tomography. J Nucl Med 1991;32:1730–7.
18. Hurst PL, Lovell-Smith CJ. Optimized assay for serum angiotensin-converting enzyme activity. Clin Chem 1981;27:2048–52.
19. Femia FJ, Maresca KP, Hillier SM, et al. Synthesis and evaluation of a series of 99mTc(CO)3+ lisinopril complexes for in vivo imaging of angiotensin-converting enzyme expression. J Nucl Med 2008;49:970–7.
20. Neels HM, Scharpe SL, Van Sande ME, Verkerk RM, Van Acker KJ. Improved micromethod for assay of serum angiotensin converting enzyme. Clin Chem 1982;28:1352–5.
21. Livak KJ, Schmittgen TD. Analysis of relative gene expression data using real-time quantitative PCR and the 2-ΔΔCT method. Methods 2001;25:402–8.
22. Hooper NM, Turner AJ. An ACE structure. Nat Struct Biol 2003;10:155–7.
23. Coates D. The angiotensin converting enzyme (ACE). Int J Biochem Cell Biol 2003;35:769–73.
24. Dzau VJ, Bernstein K, Celermajer D, et al. Pathophysiologic and therapeutic importance of tissue ACE: a consensus report. Cardiovasc Drugs Ther 2002;16:149–60.
25. Perich RB, Jackson B, Johnston CI. Structural constraints of inhibitors for binding at two active sites on somatic angiotensin converting enzyme. Eur J Pharmacol 1994;266:201–11.
26. Unger T, Gohlke P. Converting enzyme inhibitors in cardiovascular therapy: current status and future potential. Cardiovasc Res 1994;28:146–58.
27. Verjans JWH, Lovhaug D, Narula N, et al. Noninvasive imaging of angiotensin receptors after myocardial infarction. J Am Coll Cardiol Img 2008;1:354–62.
28. Van den Borne SW, Isobe S, Verjans JW, et al. Molecular imaging of interstitial alterations in remodeling myocardium after myocardial infarction. J Am Coll Cardiol 2008;52:2017–28.
29. Van den Borne SWM, Isobe S, Zandbergen R, et al. Molecular imaging for efficacy of pharmacologic intervention in myocardial remodeling. J Am Coll Cardiol Img 2009;2:187–98.
30. Verjans JW, Wolters S, Laufer W, et al. Early molecular imaging of interstitial changes in patients after myocardial infarction: comparison with delayed contrast-enhanced magnetic resonance imaging. J Nucl Cardiol 2010;17:1065–72.
31. Nahrendorf M, Hu K, Frantz S, et al. Factor XIII deficiency causes cardiac rupture, impairs wound healing, and aggravates cardiac remodeling in mice with myocardial infarction. Circulation 2006;113:1196–202.
32. Nahrendorf M, Aikawa E, Figueiredo JL, et al. Transglutaminase activity in acute infarcts predicts healing outcome and left ventricular remodelling: implications for FXIII therapy and antithrombin use in myocardial infarction. Eur Heart J 2008;29:445–54.
33. Garg R, Yusuf S; for the Collaborative Group of ACE Inhibitor Trials. Overview of randomized trials of angiotensin-converting enzyme inhibitors on mortality and morbidity in patients with heart failure. JAMA 1995;273:1450–6.
34. Giles TD, Katz R, Sullivan JM, et al. Short-and long-acting angiotensin-converting enzyme inhibitors: a randomized trial of lisinopril versus captopril in the treatment of congestive heart failure. J Am Coll Cardiol 1989;13:1240–7.
35. Foy SG, Crozier IG, Turner JG, et al. Comparison of enalapril versus captopril on left ventricular function and survival 3 months after acute myocardial infarction (the "PRACTICAL" study). Am J Cardiol 1994;73:1180–6.
36. Wienbergen H, Schiele R, Gitt A, et al. Impact of ramipril versus other angiotensin-converting enzyme inhibitors on outcome of unselected patients with ST-elevation acute myocardial infarction. Am J Cardiol 2002;90:1045–9.
37. Pilote L, Abrahamowicz M, Rodrigues E, et al. Mortality rates in elderly patients who take different angiotensin-converting enzyme inhibitors after acute myocardial infarction: a class effect? Ann Intern Med 2004;141:102–12.
38. Pilote L, Abrahamowicz M, Eisenberg M, Humphries K, Behlouli H, Tu JV. Effect of different angiotensin-converting-enzyme inhibitors on mortality among elderly patients with congestive heart failure. Can Med Assoc J 2008;178:1303–11.
39. Bacharach SL. Positron Emission Tomography. 2nd Ed. In: Dilsizian V, Pohost GM, editors. Cardiac CT, PET, and MR. Hoboken, NJ: Wiley-Blackwell, 2010:3–29.
40. Kitsiou AN, Bacharach SL, Bartlett ML, et al. ^{13}N-Ammonia myocardial blood flow and uptake: relation to functional outcome of asynergic regions after revascularization. J Am Coll Cardiol 1999;33:678–86.
41. Perrone-Filardi P, Bacharach SL, Dilsizian V, et al. Clinical significance of reduced regional myocardial glucose uptake in regions with normal blood flow in patients with chronic coronary artery disease. J Am Coll Cardiol 1994;23:608–16.

Key Words: angiotensin-converting enzyme ■ heart failure ■ lisinopril ■ radionuclide imaging ■ remodeling ■ SPECT-CT.